2015 Tenth International Conference on Ecological Vehicles and Renewable Energies (EVER)

An Overview of Analytical Methods for Magnetic Field Computation

Mitrofan Curti, Johannes J. H. Paulides, and Elena A. Lomonova
Eindhoven University of Technology
Eindhoven, 5600 MB
The Netherlands
Email: M.Curti@tue.nl, J.J.H.Paulides@tue.nl, E.Lomonova@tue.nl

***Abstract*—In this paper, several of analytical methods for modelling the magnetic field are described. These models are used in design routines of the rotating machines, linear motors as well as actuators. Thanks to their high accuracy and low requirements for computation power, they are successfully implemented in designing high precision machines. In order to enlarge the applicability of the methods it is a common practise to combine two or more model such as Magnetic Equivalent Circuit (MEC) and Harmonic Method (HM), Schwartz Christoffel (SC) mapping and Tooth Contour Method (TCM), those combinations turns into so called Hybrid Methods which are also intended to increase the computation speed and results precision.**

***Keywords*—analytical method, magnetic field, finite element analysis, equivalent circuit**

I. Introduction

Finite Element Analysis (FEA) advantages have enlarged the designing possibilities not only in magnetic field computation but also in other fields where the quantities to be modelled are distributed in space and meshed structures simplify the task. Available commercial FEA tools are of big help in most engineering problems, however in many cases the high intuitive FEA software interfaces allow the engineers lacking the knowledge of physics of the problem to blindly use the tool without knowing its limitations and therefore the problem becomes ill defined [1].

Finite Element Method (FEM) is also widely applied in electrical machines, however for electrical to mechanical energy conversion process or optimisation problems the simulations may take extremely long and the designing process may become inefficient [2]. Therefore the analytical models are rather welcome in those cases. Moreover, a properly chosen method to a specific problem [3]–[7], gives good results and in many cases precise field distribution that could allow the calculation of the forces distribution, which in case of FEA could become an issue.

Apart from numerous advantages that analytical methods have, they are usually problem dependent, therefore in order to widen the application fields they are combined by forming so called hybrid methods [8]–[11], those are usually faster and more precise. In this paper a brief description of several popular methods are presented, each of those are referred with relevant papers which use the analytical methods in specific application.

II. Theoretical background

Despite the fact that each magnetic field modelling technique, numerical or analytical, have different approaches to the problem, they still start from the same theoretical background. As it can be seen from Fig. 1, the Maxwell's equations in magnetostatic analysis are the basics for all methods. The Poisson equation, widely used in numerical methods, is the key mathematical tool to model the field of the topologies expanded in Fourier series. MEC and TCM are using integral form of Ampere's law, which in discrete form can be adjusted to second Kirchhoff's law. With free space Green function, the potential which comes from equivalent current or magnetic charge sources can be modelled. The exception makes conformal mapping methods which are used to model vector fields of all kinds. In this paper SC-mapping, which can be together with TCM for finer reluctance computation, is described in [12].

The Maxwell's equations are coupled by time varying quantities, therefore magnetostatic analysis assumes that any d/dt quantity is zero. This assumption decouples the equations and allows calculations for separated magnetic and electric field. Keeping all assumptions in mind, the potentials are equally important for field modelling, for this reason their derivation is briefly presented bellow and referred in coming sections [13].

978-1-4673-6785-1/15/$31.00

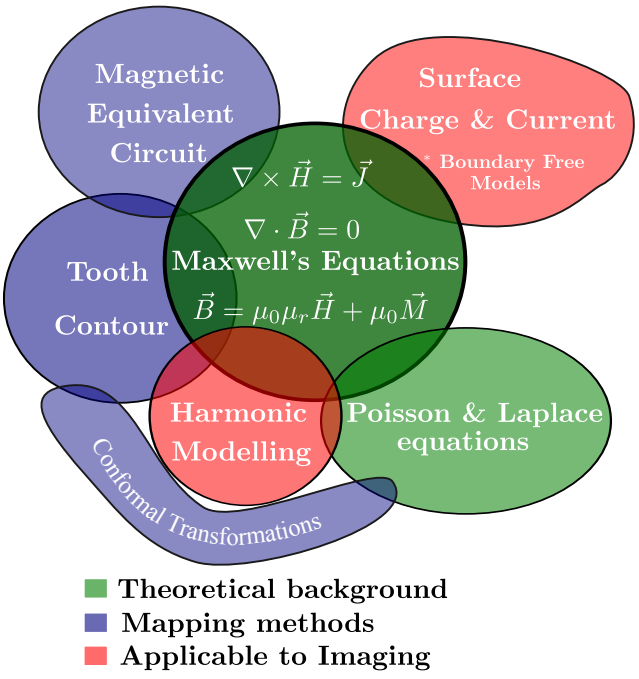

Fig. 1. Schematic representation of analytical models interconnection

A. Vector potential

In magnetostatic analysis the Gauss law for magnetisation states that $\nabla \cdot \vec{B} = 0$, where $\vec{B}$ is the vector field of the flux density, therefore the curl of magnetic vector potential $\vec{A}$ will express the same magnetic field:

$$\vec{B} = \nabla \times \vec{A}. \tag{1}$$

By substituting (1) in constitutive relation [13], we get:

$$\nabla \times \vec{A} = \mu_0\mu_r\vec{H} + \mu_0\vec{M}, \tag{2}$$

where μ_0 and μ_r are vacuum and relative magnetic permeability, $\vec{H}$ is the magnetic intensity vector field and $\vec{M}$ is the magnetisation.

By applying the Ampere's law and Coulomb gauge with condition $\left(\nabla \cdot \vec{A} = 0\right)$, the Poisson equation for the magnetic vector potential is:

$$\nabla^2\vec{A} = -\mu_0\mu_r\vec{J} - \mu_0\nabla \times \vec{M}, \tag{3}$$

where J is current density.

B. Scalar Potential

It is sometimes necessary to model magnetic field in current free regions, $\vec{J} = 0$. Taking into account that for magnetic scalar potential – $\nabla \times (\nabla\phi) = 0$, it is also true that:

$$\vec{H} = -\nabla\phi. \tag{4}$$

By substituting (4) in constitutive relation the Poisson equation for the magnetic scalar potential is obtained:

$$\nabla^2\phi = -\nabla \cdot \vec{M}_0. \tag{5}$$

Contrary to the magnetic vector potential, the solution remains a scalar regardless of the 2D or 3D problem [14].

III. Mapping Methods

One of the approaches for modelling magnetic field is mapping into more convenient maps such as equivalent circuits or complex mapping, where applied laws are similar to Maxwell's or (3), but the problem is explicitly defined and has an analytical solution.

A. Equivalent Circuit Mapping

1) Magnetic Equivalent Circuit: MEC is the first historical step to solve magnetic circuits [8]. It has been noticed that the components of a magnetic and electrical circuits have similar properties, in a way that the same laws implemented for electrical circuits could be used for magnetic circuits. For example the magnetic reluctance $\mathcal{R}$ is the analog of the electrical resistance and can be computed as:

$$\mathcal{R} = \int_L \frac{\mathrm{d}l}{\mu_0\mu_r(l)S(l)}, \tag{6}$$

where $\mu_0\mu_r$ is the magnetic permeability which in case of the resistor, in (6) it would be replaced by the inverse of resistivity $1/\rho$ and S is crossection area of the space with the length $\mathrm{d}l$. The geometry from Fig. 2 is periodic from left to right, therefore for any closed loop of N branches with reluctances or magnetomotive forces $\mathcal{F}$, an analogous to Kirchhoff law apply:

$$\sum_{k=1}^{N} H_k \cdot l_k = \sum_{k=1}^{N} \mathcal{F}_k, \tag{7}$$

where on the left H_k is the magnetic field strength over the path with the length l_k. The Equation 7 if written considering $l_k \to \infty$ results in Ampere-Maxwell law in integral form with the electric flux density $\partial D/\partial t = 0$:

$$\oint_C \vec{H}\mathrm{d}l = \int_S J_z\mathrm{d}s, \tag{8}$$

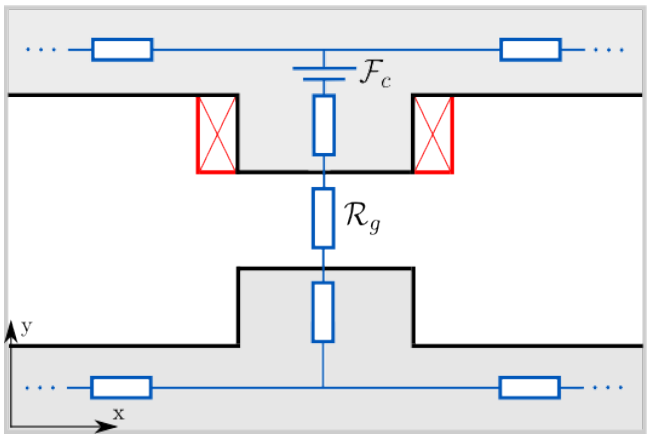

Fig. 2. Example of magnetic equivalent circuit

From Fig. 2 it can be seen that no precise results can be obtained from a similar model. However, for a higher precision a reluctance network model could be implemented [8], [15].

MEC is one of the fastest analytical method, even if it gives rough results for magnetic field distributions, it is still widely used by increasing the reluctance network members or combining MEC with other methods [10], moreover MEC method can also take into account saturation effects of materials [16], and yet, by introducing flux tubes and volumetric reluctance it gives a easiest physical understanding for magnetic field.

2) Tooth Contour Method: A hybrid combination of precise computation of reluctances (with FEM for example) is implemented in TCM, as a result the problem becomes similar to MEC [14], and allows solving it for different reluctance networks. The principle of reluctances calculation is different from MEC, where they are computed with the respect to geometrical approximations [9], [17] whereas with TCM the reluctances are computed separately for each combinations of Tooth Contours (TC), as illustrated in Fig. 3. In this case it is possible to obtain more accurate distribution of the field.

The boundaries that separate the domains with different permeability are divided in TC by means of equipotential regions. The contours are connected one to each other by reluctances, in such a way, for each rotor position, the network should be computed separately. The field is computed for each combination of TC and the final result is the sum of all local fields over these permeances. In order to have more accurate model, the TCM is especially used together with other methods like FEM, or SC mapping which will precisely estimate the reluctances [8], [11].

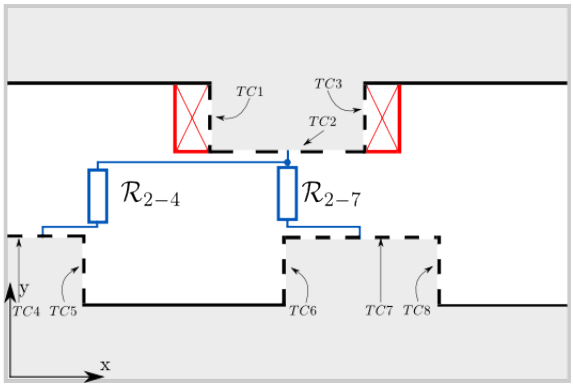

Fig. 3. Example of reluctance network for tooth contour method

B. Schwartz Christoffel Mapping

The Schwartz - Christoffel transformation allows mapping of a domain which can be bounded by a contour of any shape, onto a polygon. Therefore, this method is applicable in the fields [18], [19], where the physical quantities are homogeneously distributed in the isotropic space, and the changes in the boundaries or presence of other objects that alter the isotropy, lead to redistribution of those physical quantities.

The mathematical function which converts a complex ω-domain to another z-complex domain is:

$$S = A + C \int_{z_0}^{z} \prod_{k=1}^{n-1} (\zeta - z_k)^{\alpha_k - 1} \mathrm{d}\zeta, \tag{9}$$

where A and C are complex constants and $z_0 < z_1 < \cdots < z_{n-1}$ are real numbers satisfying $S(z_k) = \omega_k$ for $k = 1, ...n-1$ and α_k are the interior angles of the z_k vertices. For a polygon with maximum 3 vertices the mapping can be calculated explicitly, however for more vertices, the function becomes a parameter problem which can be solved only numerically [8]. For a numerical solution a MATLAB toolbox is available [20].

Therefore, with the SC toolbox it is possible to model the flux lines in the airgap geometry. For this purpose it is necessary to consider the airgap boundaries (Fig. 4 a)), to build the polygon in complex coordinates (Fig. 4 b)). In this case the mapping is performed to a rectangle which will have vertices $1, 8, 9$ and 14 with a right interior angle, whereas the rest vertices will have straight angle. The mapping result is illustrated in (Fig. 4 c)).

SC-Mapping seems to show good results compared with FEM with an error of $2-3\%$ [14]. Another advantage of SC-Mapping is that it can be easily implemented in TCM for computation of the reluctances, for instance if there is to compute the reluctance between contours

$12-11$ and $5-6$ from (Fig. 4 b)), that can be easily done by considering vertices $5, 6, 11$ and 12 having an interior right angle.

However, the method is limited to 2D problems and in most cases it will be implemented by considering infinite permeability of the core, furthermore, it is not possible to compute the field inside the core as the mapping is performed in the airgap region. Since the problem is solved numerically, it has also numerical issues such as elongation (high length to width ratios), crowding (very small distances between vertices in mapped polygon) or increasing computation time with the number of vertices [14].

IV. The Harmonic Method

The Harmonic Method is based on Poisson equation solution for orthogonal boundaries. The available solution can be obtained as Fourier series. Therefore, the investigated topology is then divided into appropriate number of orthogonal domains, as an example in Fig. 5 the topology is divided into three domains having constant permeability. Most of the electrical machines have a periodic distribution for sources, either permanent magnets (PM) or current regions, in this way it is possible to expand the sources as Fourier series:

$$\vec{S}^{(k)}(x) = \vec{S}_0^{(k)} + \sum_{n=1}^{N} \left[\vec{S}_{s_n}^{(k)} sin\left(\omega_n^{(k)} x\right) + \vec{S}_{c_n}^{(k)} cos\left(\omega_n^{(k)} x\right) \right], \tag{10}$$

Where $\vec{S}$ stands for the PM or current source for $k-$th domain, note that for problems that are solved only on the x, y plane, for the current source is considered only z component. For example from Fig. 5 the Poisson equation for source regions and Laplace for source free regions [14] will be written as:

$$\begin{aligned} \nabla^2 A_{zI} &= 0; \\ \nabla^2 A_{zII} &= -\mu_0 \nabla \times \vec{M}; \\ \nabla^2 A_{zIII} &= 0; \end{aligned} \tag{11}$$

The solution for the Poisson equation is obtained by technique of separation of variables [14]. For each domain, the boundary conditions are used to create a system of linear equations which will find the harmonic constants. The applications of HM method [5], [6], [21] shows a good agreement with the FEM method moreover, the simulation time is two orders shorter than with FEM, which makes HM powerful tool for optimisation and transient states modelling, HM is also recognised in

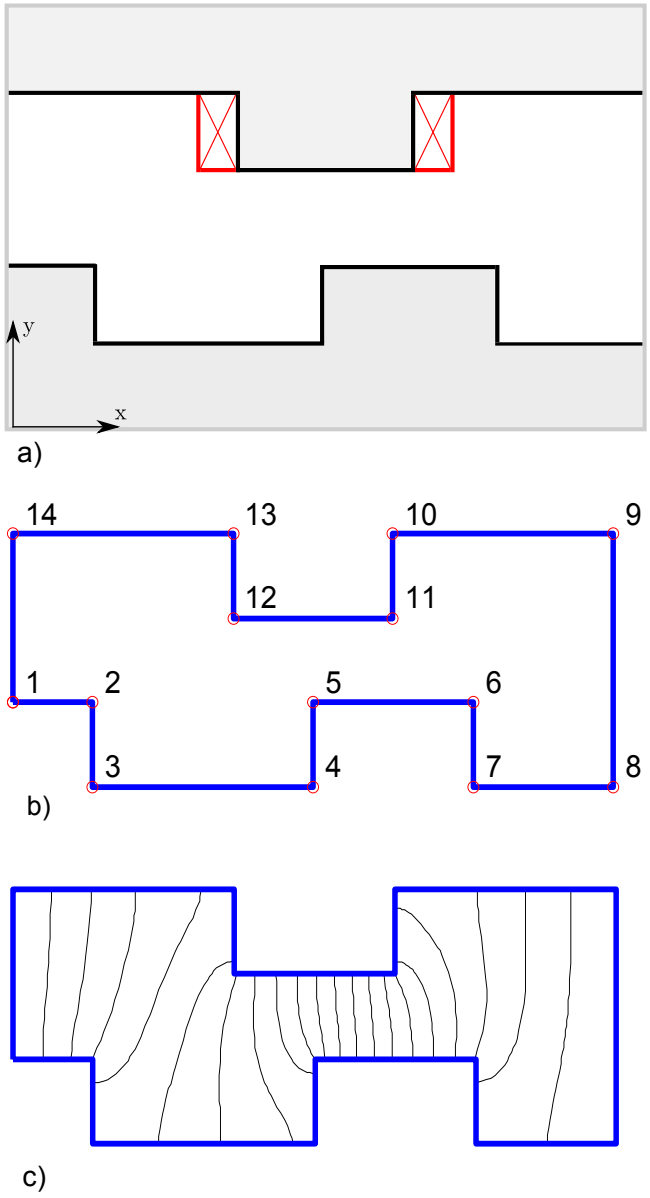

Fig. 4. Schwartz - Christoffel mapping for slotted structure, a) The slotted structure geometry in polar coordinates, b) Equivalent polygon ready to be mapped, c) Result of SC mapping from a rectangular shape

many publications as one of the best choices. Like every analytical method, HM is problem dependent, However some tools are being developed to interface the computational method with the user. Another issue is tacking into account the infinite permeability of the iron. Therefore is not possible to model the field inside it. However, few attempts of taking into account a linear μ encountered success [22], and another publication, in which the slotting region is expanded into Fourier series, is in the press.

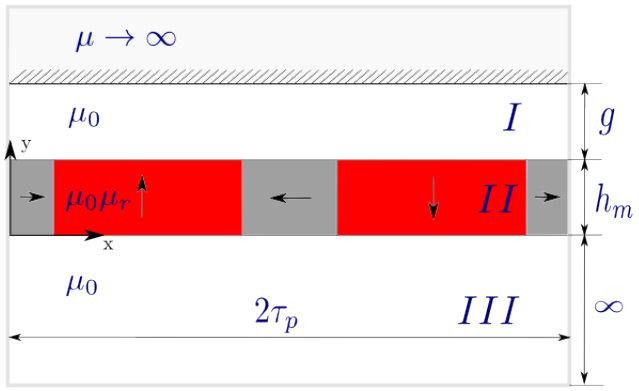

Fig. 5. Linear Actuator Topology adopted for Harmonic Model

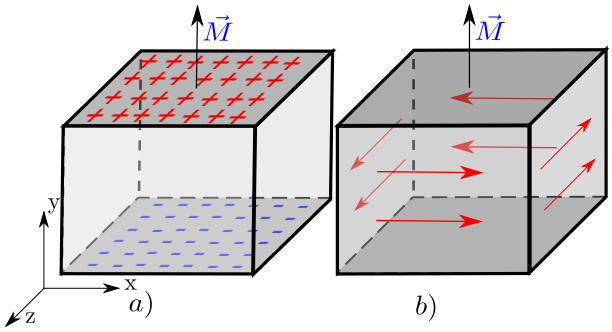

Fig. 6. Explicative to equivalent charge a), and current sheets b).

V. Surface Charge and Current Models

The Surface Charge and Current Models give an analytical 2D or 3D solution for the magnetic field in free space. Therefore it is suitable for modelling PMs in free space or surrounded by materials with μ_r close to 1. Another advantage of those models is that there is no necessity for formulating boundary problems. By considering $\mu_r \approx 1$ it allows to use superposition principle to model the field coming form multiple sources. However, there are already attempts to include the finite permeability by finding the exact distribution of the magnetic charges on the magnet surface, but still a part of the solving process contains iterative computation [23], [24].

The surface charge model places fictitious equivalent magnetic charges on the surfaces of the PMs using scalar potential, whereas surface current model places a curl of equivalent current sheet around the magnet using vector potential [25].

A. Current Model

If (3) is written in integral form using the free-space Green's function we get:

$$\vec{A}(\vec{x}) = \frac{\mu_0}{4\pi}\int\limits_V \frac{\vec{J}_m(\vec{x}')}{|\vec{x}-\vec{x}'|}\mathrm{d}v' + \frac{\mu_0}{4\pi}\int\limits_S \frac{\vec{j}_m(\vec{x}')}{|\vec{x}-\vec{x}'|}\mathrm{d}s', \quad (12)$$

Where the volume and surface current density is $\vec{J}_m = \nabla \times \vec{M}$ and respectively $\vec{j}_m = \vec{M} \times \vec{n}$. In most of the cases the magnetisation of the permanent magnets is homogeneously distributed and the curl of magnetisation inside the magnet is null, however the surface current density is distributed as in Fig. 6 b). In this way we get the relationship for $\vec{B}$ field:

$$\vec{B}(\vec{x}) = \frac{\mu_0}{4\pi}\int\limits_S \vec{j}_m(\vec{x}')\frac{\vec{x}-\vec{x}'}{|\vec{x}-\vec{x}'|^3}\mathrm{d}s', \quad (13)$$

Equation 13 is modelling the field from an equivalent surface current distributed on lateral surfaces of the PM.

B. Charge Model

The same principle as for Current Model holds for scalar potential, therefore (5) is written using free space Green's function:

$$\phi = -\frac{1}{4\pi}\int\limits_V \frac{\rho_m(\vec{x}')}{|\vec{x}-\vec{x}'|}\mathrm{d}v' + \frac{1}{4\pi}\oint\limits_S \frac{\sigma_m(\vec{x}')}{|\vec{x}-\vec{x}'|}\mathrm{d}s', \quad (14)$$

Where volume and surface charge density are $\rho_m = \nabla \cdot \vec{M}$ and respectively current density $\sigma_m = \vec{M} \cdot \vec{n}$. For the same homogeneity reasons the modelled field is only from the surface density placed on top and bottom of the PM, as shown in (Fig. 6 a)), therefore:

$$\vec{B}(\vec{x}) = \frac{\mu_0}{4\pi}\int\limits_S \sigma_m(\vec{x}')\frac{\vec{x}-\vec{x}'}{|\vec{x}-\vec{x}'|^3}\mathrm{d}s', \quad (15)$$

For simplicity matters it is often preferable to choose Charge Model, as it is always simpler to model 2 surfaces instead of 4 [25].

VI. Method of Images

Imaging is not a modelling method by itself, but in combination with other methods is of good help. It is especially suitable when the sources are close to the iron (boundaries) compare to thickness of the iron itself. By modelling the field of the both imaged and real sources it will be possible to apply the principle of superposition as the assumption is that all sources are in the domains with the same μ_r, however relevant results are only those from the domain of real source [25], [26].

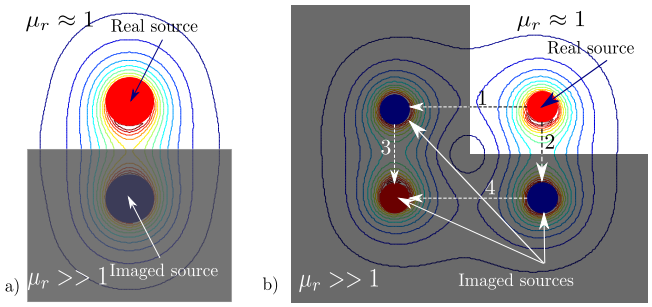

Fig. 7. Explicative to Method of images: a) Flat boundary b) Right angle boundary.

When the problem has more complex boundaries than flat [4], (Fig. 7 a)) and right angle boundaries (Fig. 7 b)), the construction of the images becomes more sophisticated, or in case of one source between two parallel boundaries an infinite amount of images has to be taken into account. However with this method it is possible to take into account the finite permeability, in that case the values for the imaged sources become:

$$I' = -\frac{\mu_r - 1}{\mu_r + 1} I. \tag{16}$$

VII. Conclusion

An overview of analytical methods for magnetic field modelling has been briefly described in this paper. Depending on the purpose, a proper analytical model should be chosen. For example, some rough approximations could be made with fast MEC model and afterwards, at the final stage of the design process, a more precise model could be used for final refinements. With a more dense reluctance network, MEC as well as TCM gives more precise results as the concentrated elements represent the physical quantities from a smaller unity of space. SC-mapping, an universal field solver, can be also used together with TCM for reluctance computation. More advanced methods, that give precise information about field distribution, and therefore distribution of forces, are HM and surface charge and current methods.

HM which solves Poisson and Laplace equations for separated regions of a periodic topology, is widely implemented in designing tools, however the consideration of finite and linear permeability is still under development and ignoring saturation or including boundary condition make them inapplicable for machines where high saturation occurs or end effects are significantly altering the results.

Surface charge or current are suitable for field modelling in free space, furthermore those methods are boundary free, therefore the results are not affected by boundary conditions, however the relative permeability of the materials should be chosen close to 1. For consideration of $\mu_r > 1$ the method of images could be implemented with an yet iterative computation of precise magnetic surface charge distribution.

Acknowledgment

This paper is part of the ADvanced Electric Powertrain Technology (ADEPT) project which is an EU funded Marie Curie ITN project, grant number 607361. Within ADEPT a virtual and hardware tool are created to assist the design and analysis of future electric propulsions. Especially within the context of the paradigm shift from fuel powered combustion engines to alternative energy sources (e.g. fuel cells, solar cells, and batteries) in vehicles like motorbikes, cars, trucks, boats, planes. The design of these high performance, low cost and clean propulsion systems has stipulated an international cooperation of multiple disciplines such as physics, mathematics, electrical engineering, mechanical engineering and specialisms like control engineering and safety. By cooperation of these disciplines in a structured way, the ADEPT program provides a virtual research lab community from labs of European universities and industries [1].

[1] A. Stefanskyi, A. Dziechciarz, F. Chauvicourt, G. E. Sfakianakis, K. Ramakrishnan, K. Niyomsatian, M. Curti, N. Djukic, P. Romanazzi, S. Ayat, S. Wiedemann, W. Peng, S. Sjipetic, Researchers within the EU funded Marie Curie ITN project ADEPT, grant number 607361, 2013-2017.

References

[1] C. W. Eckard, "Advantages and disadvantages of fem analysis in an early state of the design process," 2014.

[2] J. W. Jansen, J. P. C. Smeets, T. T. Overboom, J. M. M. Rovers, and E. A. Lomonova, "Overview of analytical models for the design of linear and planar motors," *Magnetics, IEEE Transactions on*, vol. 50, no. 11, pp. 1–7, Nov 2014.

[3] M. Kovacic, Z. Hanic, S. Stipetic, S. Krishnamurthy, and D. Zarko, "Analytical wideband model of a common-mode choke," *Power Electronics, IEEE Transactions on*, vol. 27, no. 7, pp. 3173–3185, July 2012.

[4] K. J. W. Pluk, T. A. van Beek, J. W. Jansen, and E. A. Lomonova, "Modeling and measurements on a finite rectangular conducting plate in an eddy current damper," *Industrial Electronics, IEEE Transactions on*, vol. 61, no. 8, pp. 4061–4072, Aug 2014.

[5] R. L. J. Sprangers, B. L. J. Gysen, J. J. H. Paulides, and E. A. Lomonova, "A fast semi-analytical model for the slotted structure of induction motors with 36/28 stator/rotor slot combination," in *ELECTRIMACS 2014*, May 2014.

[6] R. L. J. Sprangers, B. L. J. Gysen, J. J. H. Paulides, J. Waarma, and E. A. Lomonova, "Calculation of induced rotor current in induction motors using a slotted semi-analytical harmonic model," in *Power Electronics and Applications (EPE'14-ECCE Europe), 2014 16th European Conference on*, Aug 2014, pp. 2700–2705.

[7] J. L. G. Janssen, B. L. J. Gysen, J. J. H. Paulides, and E. A. Lomonova, "Advanced electromagnetic modeling applied to anti-vibration systems for high precision and automotive applications," *International Compumag Society Newsletter*, vol. 19, no. 1, pp. 3–16, 2012.

[8] E. Ilhan, "Hybrid modeling techniques embracing permanent-magnet-biased salient machines," Ph.D. dissertation, Eindhoven University of Technology, Nov. 2014.

[9] E. Ilhan, J. J. H. Paulides, L. Encica, and E. A. Lomonova, "Tooth contour method implementation for the flux-switching pm machines," in *Electrical Machines (ICEM), 2010 XIX International Conference on*, Sept 2010, pp. 1–6.

[10] E. Ilhan, B. L. J. Gysen, J. J. H. Paulides, and E. A. Lomonova, "Analytical hybrid model for flux switching permanent magnet machines," *Magnetics, IEEE Transactions on*, vol. 46, no. 6, pp. 1762–1765, June 2010.

[11] E. Ilhan, M. F. J. Kremers, E. T. Motoasca, J. J. H. Paulides, and E. A. Lomonova, "Spatial discretization methods for air gap permeance calculations in double salient traction motors," *Industry Applications, IEEE Transactions on*, vol. 48, no. 6, pp. 2165–2172, Nov 2012.

[12] K. J. Binns, P. J. Lawrenson, and C. W. Trowbridge, *The analytitcal and numerical solution of electric and magnetic fields*. John Wiley & Sons, 2001.

[13] E. P. Furlani, *Electric Machines and Drives*, I. Mayergoyz, Ed. Acadenic Press, 2001.

[14] D. C. J. Krop, "Integration of Dual Electromagnetic Energy Conversions," Ph.D. dissertation, Eindhoven University of Technology, 2013.

[15] S. Ouagued, Y. Amara, and G. Barakat, "Comparison of hybrid analytical modelling and reluctance network modelling for predesign purposes," 2014.

[16] A. Sari, C. Espanet, D. Chamagne, F. Lanzetta, D. Marquet, and P. Nika, "Reluctance network modeling tubular linear alternator considering iron nonlinearities," in *Electrical Machines and Systems, 2009. ICEMS 2009. International Conference on*, Nov 2009, pp. 1–6.

[17] H. C. Roters, *Electromagnetic Devices*. John Wiley & Sons, 1958.

[18] P. P. Bergonio, "Schwarz-Christoffel Transformations," Master's thesis, 2007.

[19] H. Chanson, *Theorem of Schwartz - Christofell, Free Streamlines & Applications*, QLD 4072, Oct. 2007.

[20] T. A. Driscoll, *Schwarz–Christoffel Toolbox User's Guide*.

[21] R. L. J. Sprangers, J. J. H. Paulides, B. L. J. Gysen, E. A. Lomonova, and J. Waarma, "Electric circuit coupling of a slotted semi-analytical model for induction motors based on harmonic modeling," in *Energy Conversion Congress and Exposition (ECCE), 2014 IEEE*, Sept 2014, pp. 1301–1308.

[22] K. J. W. Pluk, G. De Gersem, J. W. Jansen, and E. A. Lomonova, "Fourier modeling of magnetic shields with linear permeable material and finite dimensions," *Magnetics, IEEE Transactions on*, vol. 49, no. 7, pp. 4160–4163, July 2013.

[23] D. T. E. H. van Casteren, J. J. H. Paulides, and E. A. Lomonova, "3-d numerical surface charge model including relative permeability: The general theory," *Magnetics, IEEE Transactions on*, vol. 50, no. 11, pp. 1–4, Nov 2014.

[24] D. T. E. H. van Casteren, J. J. H. Paulides, and E. A. Lomonova, "3-d semianalytical surface charge model including relative permeability using polynomial approximation," *Magnetics, IEEE Transactions on*, vol. 50, no. 11, pp. 1–4, Nov 2014.

[25] J. L. G. Janssen, "Extended Analytical Charge Modeling for Permanent-Magnet Based Devices," Ph.D. dissertation, Eindhoven University of Technology, Dec. 2011.

[26] B. Hague, *The Principles of Electromagnetism*. Dover Publications, 1962.